A Single Stage Photovoltaic System For A Dual Inverter-Fedopen-End Winding Induction Motor Drive For Pumping Applications

1.K.ROHIT KRISHNA,2. C. BALA CHANDRA REDDY ,Associate professor & HOD
1,2.Department of EEE, CHILKUR BALAJI INSTITUTE OF TECHNOLOGY,Hyderabad

Abstract ***This paper presents an integrated solution for a photovoltaic (PV)-fed water-pump drive system, which uses an open end winding induction motor (OEWIM). The dual-inverter-fed OEWIM drive achieves the functionality of a three-level inverter and requires low value dc-bus voltage. This helps in an optimal arrangement of PV modules, which could avoid large strings and helps in improving the PV performance with wide bandwidth of operating voltage. It also reduces the voltage rating of the dc-link capacitors and switching devices used in the system. The proposed control strategy achieves an integration of both maximum power point tracking and V/f control for the efficient utilization of the PV panels and the motor. The proposed control scheme requires the sensing of PV voltage and current only. Thus, the system requires less number of sensors. All the analytical, simulation, and experimental results of this work under different environmental conditions are presented in this paper.***

Index Terms—Centrifugal pump, dual-inverter, maximum power point tracking (MPPT), open-end winding induction motor (OEWIM), photovoltaic (PV) cell.

I.INTRODUCTION

Electrical motors constitute more than 40% of total electric power consumption [1]. Modernization of human society and growing applications of electric motors have exponentially increased the demand for electrical energy. This forces an increase in the power generation capacity. However, due to ecological concerns, restriction and constraints are imposed on increasing the generation capacity of conventional sources. So, contemporary research is focused toward an effective utilization of nonconventional energy sources. Among the available nonconventional sources, photovoltaic (PV) technology seems to be the most promising and attractive. This can be attributed to declining cost of PV modules, free energy source, zero maintenance, and noise free operation. Thus, employment of a PV source for powering electric motor could be a good solution especially for water-pumps, electric fans, submersible pumps, etc. Such loads can have the option of optimally using PV power whenever Sun power is available [2].

Further, when such loads are used in the stand-alone system like water pumping application in domestic, agricultural, and industrial sectors, solar PV powered system could be a good solution. It could meet the requirement during critical situation, i.e., during summer especially in tropical countries like India.

This encourages the use of electric motor-pump with better performance and efficiency with the PV system [3]. Some possible solutions given for PV-fed water-pump were based on usage of dc motor either directly coupled [4] or via a dc–dc converter [5] with the PV source. However, the requirement of continuous maintenance and higher cost restricts the use of dc motors for their application in PV water pumping systems [3]. Thus, there is a need of such a solution that uses the PV power effectively, while using a low cost, low maintenance, reliable, and robust motor for pumping application. The most suitable motor for such an application is an induction motor (IM).

Some of the initial proposals for a PV-fed IM, based on the two-stage system, were given by various authors in the past. Most of them have used a dc–dc boost converter in the first stage and the second stage comprises of a dc–ac inverter. Boost converter amplifies and operates the low value PV input voltage near maximum power point (MPP) while the inverter gives the required ac voltage to the IM. Also, the control techniques are based on either independent frequency control [2], or a *V/f* control [6]. Recently, a proposal based on closed-loop speed control to improve the performance and efficiency of the system was given by Alves Vitorino *et al*. [7], in which the authors have presented a sensor-less speed control technique. However, two stage power conversion, high voltage rating of semiconductor devices, and more number of sensors increase the power loss and cost of the system.

II.MODELING OF THE PROPOSED SYSTEM

A proposed configuration of the solar PV-powered pumping system is shown in Fig. 2, which comprises of: 1) solar PV array; 2) dual-inverter namely Inverters I and II; 3) three-phase

OEWIM with pump load; and 4) controller block which consists of MPPT and DSAZE PWM algorithm. These components are described in detail in the following sections.

PV Source Model

The PV source was modeled by using PV cell *current–voltage* characteristic equation as follows .

$$i_{pvcell} = i_L - i_0 \left(e^{\frac{q\left(v_{pvcell} + i_{pvcell} R_s\right)}{nkT}} - 1 \right) \quad (1)$$

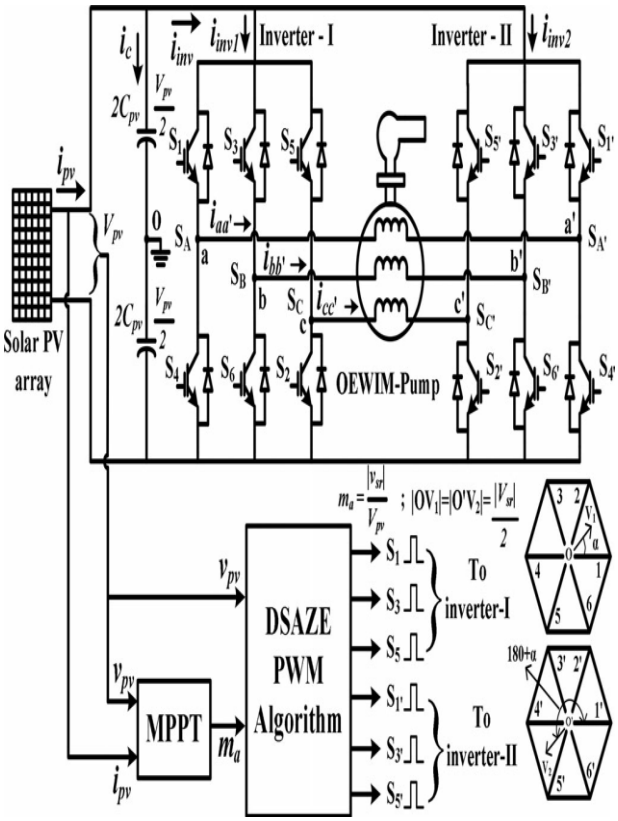

Fig. 7.1.. Schematic circuit diagram of the proposed system.

where I $_{pv\ cell}$ is PV cell current, *iL* is photocurrent, *i*0 is diode saturation current, *n* is diode quality or ideality factor, *k* is Boltzmann constant, *q* is electron charge, *T* is panel operating temperature in Kelvin, *Rs* is PV cell series resistance, and *v*pvcell is PV cell voltage (V).

The output of PV source is connected to inverter with dc-bus capacitance *Cpv* . By applying KCL at input of the inverter [from Fig. 2]

$$i_{\mathrm{pv}} = i_c + i_{\mathrm{inv}} \Rightarrow i_{\mathrm{pv}} = C_{\mathrm{pv}} \frac{dv_{\mathrm{pv}}}{dt} + i_{\mathrm{inv}} \quad (2)$$

Integral solution of (2) is the voltage *v*pv across capacitance *C*pv , which is used by the PV model to calculate the PV source current. The inverter current *i*inv is the current drawn by Inverters I and II. Further dual inverter has two series connected equal value capacitors across the dc link. These capacitors share equal voltage with respect to the common point "o" as shown in Fig. 2.

Modular Three-Level Dual-Inverter Model

Dual inverter used in the proposed configuration is modeled using switching functions [30]. To model dual inverter, switching function *SW* (where*W*can be *A*, *B*, *C*, *A'*, *B'* or *C'* depending on the phase and number of inverter) requires the logic generated from the PWM controller. The modular dual inverter shown in Fig. 2 consists of six poles (*a, b, c, a', b'*, and *c'*) and 12 switches (two switches per pole). The value of the pole voltages in a particular phase can be ±*Vpv* /2 depending on the switch (whether top or bottom) is turned ON. If top switch of phase "*a*", *S*1 is turned ON, the pole voltage *vao* is +*Vpv* /2 and when bottom switch of phase "*a*", *S*4 is turned ON, then the pole voltage *vao* is −*Vpv* /2. Thus, pole voltage of Inverter I can be given as

$$v_{ao} = S_A \frac{V_{\mathrm{pv}}}{2};\ v_{bo} = S_B \frac{V_{\mathrm{pv}}}{2};\ v_{co} = S_C \frac{V_{\mathrm{pv}}}{2} \quad (3)$$

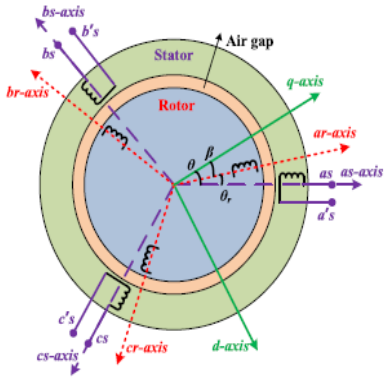

Fig. 7.3. OEWIM model.

Similarly, pole voltage of Inverter II can be given as

$$v_{a'o} = S_{A'} \frac{V_{\mathrm{pv}}}{2};\ v_{b'o} = S_{B'} \frac{V_{\mathrm{pv}}}{2};\ v_{c'o} = S_{C'} \frac{V_{\mathrm{pv}}}{2} \quad . (4)$$

The motor phase voltage *vaa*_ is given by

$$v_{aa'} = \frac{V_{\mathrm{pv}}}{2}\left[\frac{2}{3}(S_A - S_{A'}) - \frac{1}{3}((S_B - S_{B'}) + (S_C - S_{C'}))\right] \quad (5)$$

Similarly, the other phase voltages *vbb*_, *vcc*_ of the inverter output can be derived for the system. Further, the input inverter current *i*inv can also be derived using switching functions. Current flowing through Inverter I is given by

$$i_{\mathrm{inv1}} = \frac{1}{2}(S_A + 1)i_{aa'} + \frac{1}{2}(S_B + 1)i_{bb'} + \frac{1}{2}(S_C + 1)i_{cc'} \quad . (6)$$

Current flowing through the Inverter II is given by

$$i_{\mathrm{inv2}} = \frac{1}{2}(S_{A'} + 1)(-i_{aa'}) + \frac{1}{2}(S_{B'} + 1)(-i_{bb'}) + \frac{1}{2}(S_{C'} + 1)(-i_{cc'}) \quad . (7)$$

The net current flowing through the dual inverter is

$$i_{\mathrm{inv}} = \frac{1}{2} i_{aa'}(S_A - S_{A'}) + \frac{1}{2} i_{bb'}(S_B - S_{B'}) + \frac{1}{2} i_{cc'}(S_C - S_{C'}) \quad . (8)$$

Thus, the previous values of phase voltage and current can be used by the Simulink model of OEWIM, which is discussed in the next section.

OEWIM Model

An OEWIM [28] is obtained by opening the neutral point of the star-connected stator windings of a normal three-phase IM. The winding diagram of three-phase OEWIM is shown in

Fig. 3. For modeling and analysis, the decoupled form of OEWIM is considered. For transforming the stator ($\varphi = \theta$) and the rotor parameters ($\varphi = \beta$) to decoupled form, the transformation matrix used is given as follows:

$$\begin{bmatrix} x_{qy} \\ x_{dy} \\ x_{0y} \end{bmatrix}$$

$$= \frac{2}{3}\begin{bmatrix} \cos\phi & \cos(\phi-2\pi/3) & \cos(\phi+2\pi/3) \\ \sin\phi & \sin(\phi-2\pi/3) & \sin(\phi+2\pi/3) \\ 1/2 & 1/2 & 1/2 \end{bmatrix}\begin{bmatrix} x_{aa'} \\ x_{bb'} \\ x_{cc'} \end{bmatrix} \quad (9)$$

where θ is the angle between the stator *as*-axis and the quadrature (*q*) axis, β is the angle between rotor *ar*-axis and the *q*-axis, also $\beta = \theta - \theta r$, θr is the angle between rotor *ar*-axis and stator *as axis* (see Fig. 3), parameter *x* can be either voltage "*v*" or current "*i*" or flux linkage "λ" and subscript parameter *y* can be "s" or "*r*." The subscript "s" denotes the parameters of stator and the subscript "*r*" denotes the parameters of rotor.

The dynamic *d*–*q* model of an OEWIM is described by

$$v_{qs} = R_s i_{qs} + \omega\left(L_{ls} i_{ds} + L_m\left(i_{ds} + i'_{dr}\right)\right) + p\lambda_{qs} \quad (10)$$

$$v_{ds} = R_s i_{ds} - \omega\left(L_{ls} i_{qs} + L_m\left(i_{qs} + i'_{qr}\right)\right) + p\lambda_{ds} \quad (11)$$

$$v'_{qr} = R'_r i'_{qr} + \left(\omega - \omega_r\right)\left(L'_{lr} i'_{dr} + L_m\left(i_{ds} + i'_{dr}\right)\right) + p\lambda'_{qr} \quad (12)$$

$$v'_{dr} = R'_r i'_{dr} - \left(\omega - \omega_r\right)\left(L'_{lr} i'_{qr} + L_m\left(i_{qs} + i'_{qr}\right)\right) + p\lambda'_{dr} \quad (13)$$

where *R*r is rotor resistance, *R*s is stator resistance, *L*ls is stator leakage inductance, *L'*lr is rotor leakage inductance, *L*m is mutual inductance between stator and rotor winding, ω is the synchronous speed, ωr is the electrical speed of motor, and *p* denotes the time derivative. Also, here *v_qr* = *v_dr* = 0, since rotor bars are short-circuited.

The expression for the electromagnetic torque *T*em is given by

$$T_{\text{em}} = \frac{3}{2}\frac{P}{2} L_m\left[i_{qs} i'_{dr} - i_{ds} i'_{qr}\right] \quad (14)$$

where *P* is the number of poles.

III.OPERATION AND ANALYSIS OF THE PROPOSED SYSTEM

The proposed dual inverter is operated by using the decoupled PWM strategy. It incorporates simple *V/f* control for the efficient operation of system below the rated speed. The proposed PWM requires the information of magnitude and angle of the reference voltage vector. The magnitude is calculated and controlled by the MPPT algorithm and the angle "α" is the function of time and fundamental frequency of reference

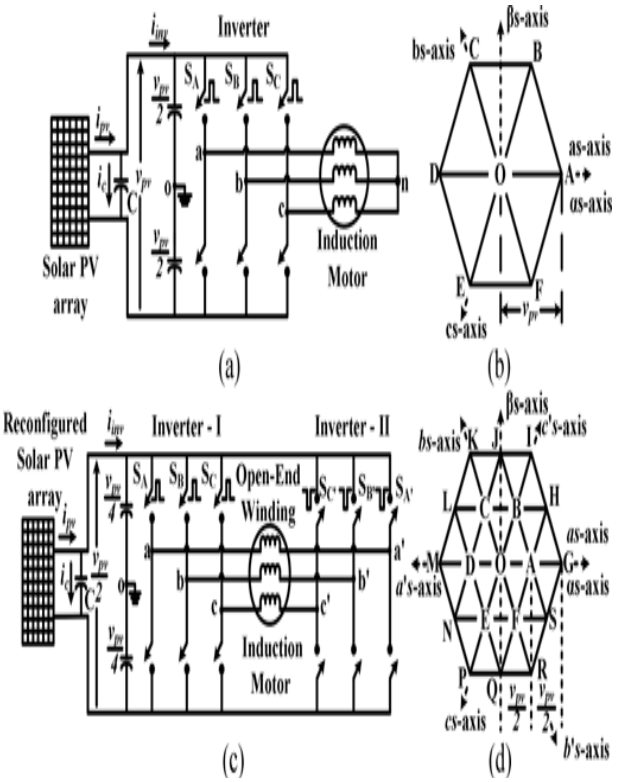

Fig. 4. Demonstration and comparison of dc-bus voltage requirement for H-bridge and dual-inverter systems. (a) Schematic circuit diagram of the two-level H-bridge inverter with input dc voltage (PV voltage) of "*V*pv ." (b) Space vector locations of voltage vector obtained from two-level inverter. (c) Schematic
circuit diagram of dual-inverter-fed OEWIM drive with input dc voltage (PV voltage) of "*Vpv* /2." (d) Space vector locations of voltage vector obtained from three-level dual-inverter scheme. Modulating waveform. The reference voltage vector |*v*sr |_α is further divided into two decoupled components |*v*sr |/2 _ α and |*v*sr |/2_(180+α). The decoupled components are then given as the reference vector for Inverters I and II, respectively, as shown in Fig. 2, for generation of required output voltage. Thus, using decoupled PWM configuration has the benefit of double output voltage.

Low Input DC-Bus Voltage Requirement of Dual Inverter for OEWIM-Pump Drive

To analytically verify the low input dc-bus voltage requirement, a comparison between two-level and dual-inverter-fed OEWIM is done. Both the inverters are compared for generating the same output voltage vector with different values of input PV source voltage. The low input voltage requirement of dual inverter for an OEWIM drive is demonstrated in Fig. 4.

Let the PV source voltage required to generate the rated instantaneous IM phase voltage *van* is *Vpv* as shown in Fig. 4(a). From Fig. 4(a) and (b), the inverter output voltage, *van* , *vbn* , and *vcn* can be obtained using the inverter pole voltage, *vao* , *vbo* , and *vco* ; and switching functions *S*A, *S*B, and *S*C as follows:

$$v_{an} = v_{ao} - v_{no} = \left(\frac{2}{3}S_A - \frac{1}{3}\left(S_B + S_C\right)\right)\frac{V_{\text{pv}}}{2} \quad (16)$$

where *vno* is common-mode voltage given by

$$v_{no} = \frac{1}{3}(v_{ao} + v_{bo} + v_{co}) = \frac{1}{3}(S_A + S_B + S_C)\frac{V_{pv}}{2} \quad (17)$$

Thus, the space vector location of reference voltage vector *OA* [see Fig. 4(b)] can be generated by the switching functions *SA* = 1, *SB* = −1, and *SC* = −1. Substituting these values into (17) will result in the phase voltage, *van* as 2*Vpv* /3.

Now, consider the three-phase, three-level dual inverter connected to an OEWIM as shown in Fig. 4(c). Let the input PV source voltage is *Vpv* /2, which is half of the voltage taken for two-level H-bridge inverter. Now, the dual inverter output phase
[see Fig. 4(d)] is given as

$$v_{aa'} = v_{ao} - v_{a'o'} - v_{oo'} \quad (18)$$

where *voo*_ is the common mode voltage [see Fig. 4(c)] which is given by

$$v_{oo'} = \frac{1}{3}\frac{V_{pv}}{4}\left[(S_A - S_{A'}) + (S_B - S_{B'}) + (S_C - S_{C'})\right] \quad (19)$$

Therefore, *vaa*_ is given by

$$v_{aa'} = \left(\frac{2}{3}(S_A - S_{A'}) - \frac{1}{3}\left[(S_B - S_{B'}) + (S_C - S_{C'})\right]\right)\frac{V_{pv}}{4} \quad (20)$$

So, to generate voltage vector
OG [see Fig. 4(d)], the switching functions required are *SA* = 1, *SB* = −1, and *SC* = −1; *SA*_ = −1, *SB*_ = 1, and *SC*_ = 1. Substituting these values in (20), results in the phase voltage of magnitude 2*Vpv* /3 corresponding to phase *aa'*.

Hence, to generate the phase voltage of 2*Vpv* /3, the PV source voltage required in case of two-level inverter is *Vpv* and in case of dual inverter connected to OEWIM is *Vpv* /2. However, the DSAZE PWM technique [22] needs excess 15% of dc-link voltage to generate the rated motor phase voltage.

CONTROL STRATEGY AND MPPT ALGORITHM:

The solar PV-powered-fed dual inverter connected to OEWIM-pump drive is operated using a simple control strategy, which simultaneously accomplishes MPPT and DSAZE PWM integrated together. This integrated algorithm generates the required PWM control signals for the modular dual inverter. The flowchart of control algorithm is shown in Fig. 5. The MPPT part of algorithm facilitates motor-pump drive to extract maximum available power from the PV source, thereby assuring effective utilization of the PV source. The DSAZE PWM part of the algorithm incorporates *V/f* control. It maintains constant rated flux in the motor which retains the maximum torque capability of the machine for the given PV power. Thus, in pump drive application where torque is proportional to square of speed, maintaining the maximum torque further helps in maximum utilization of the input source.

MPPT Algorithm

One of the simplest, most popular, and commercially used methods of MPPT, namely, the Hill Climbing algorithm [31] is employed in the proposed system. The algorithm first senses the voltage (*vpv*) and current (*ipv*) of PVarray for calculating the power (*p*pv). The calculated and sensed PV power and voltage are then compared with their previous value to determine the slope of the operating point. The considered slope then determines the correction for modulation index (*m*a).With respect to sign of the slope (negative or positive), the value of *m*a is modified (incremented or decremented) as described in the flowchart shown in Fig. 5 until the operating point reaches near MPP. The calculated value of *m*a is then used by the DSAZE PWM algorithm.

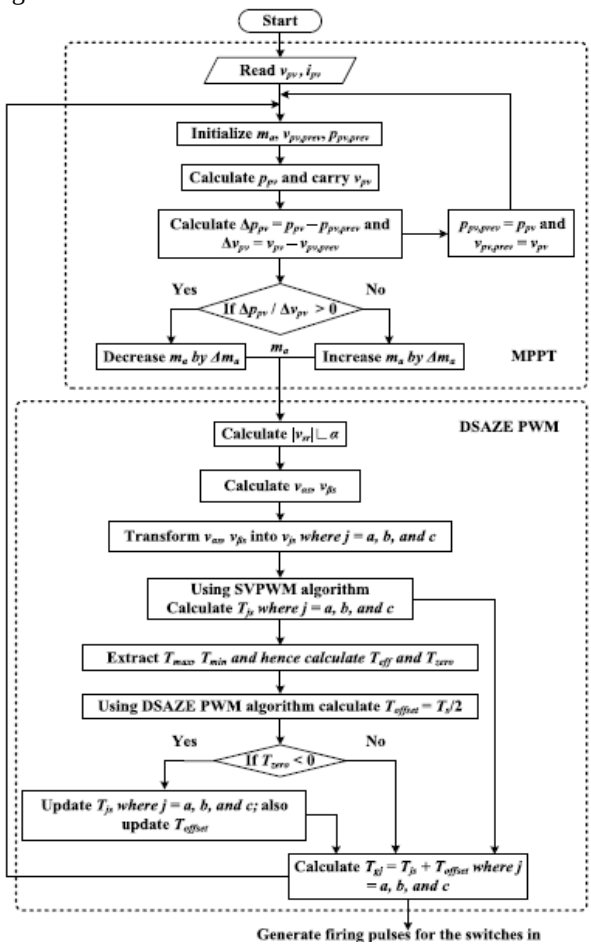

Fig. 5. Flowchart of the MPPT, DSAZE algorithm used in the proposed scheme.

B. DSAZE PWM Algorithm

The magnitude of the reference voltage vector generated by the MPPT output and angle "*α*" is decomposed into the instantaneous three-phase reference voltage *vas*, *vbs* , and *vcs* for Inverter I. The gating time *Tgj* (*j* = *a*, *b*, *c*) for top switches of Inverter I (see Fig. 2) is then obtained by the switching algorithm [32]. This algorithm [32] requires instantaneous values of the reference phase voltage for calculating the effective time (time for which all the active vectors are switched) or turned ON time for top switches. The position of effective time period can be adjusted in such a way that the offset time is equal to *Ts*/2 within a switching period. This feature is exploited by the DSAZE PWMtechnique to eliminate the zero sequence voltage within a sampling period.

As DSAZE is a center-spaced PWM technique for the dualinverter system, the ripple content in current is less and hence results in the improvement of developed torque. The other advantage of the DSAZE PWM algorithm for OEWIM drive is that it requires less memory and computing time for processing.

As both the reference voltage vectors for Inverters I and II are in the phase opposition, the gating time *Tgj_* (*j* = *a*, *b*, *c*) for the top switches of Inverter II are directly obtained using the
gating time for Inverter I as follows:

$$Tgj\_ = Ts - Tgj \qquad (21)$$

where *j* = *a*, *b*, *c* and *Ts* is the inverter switching time period(s). Complement of the respective gating signals for Inverters I and II are generated for bottom switches for both inverters.

IV.SIMULATION RESULTS

Solar input

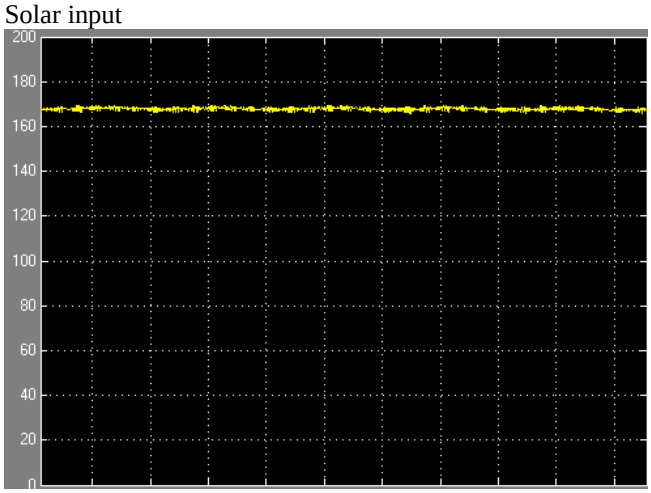

Voltage across capacitor CI

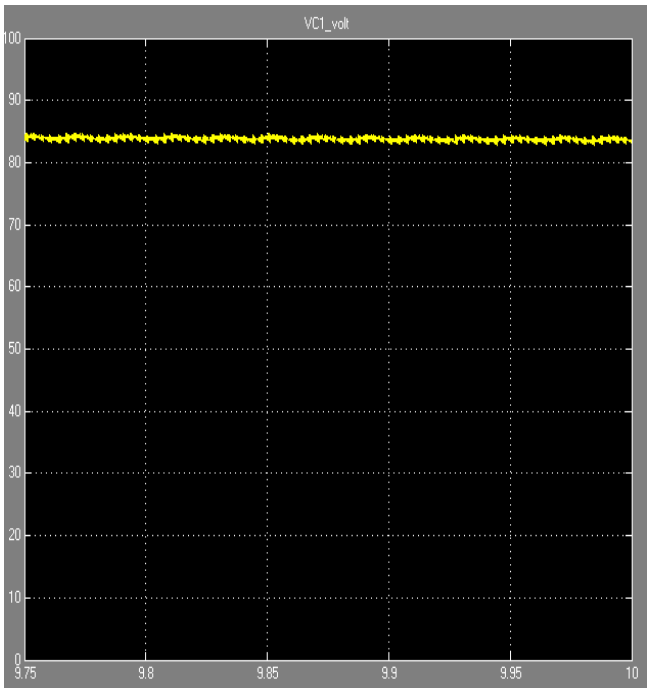

Open end winding-1 voltages:

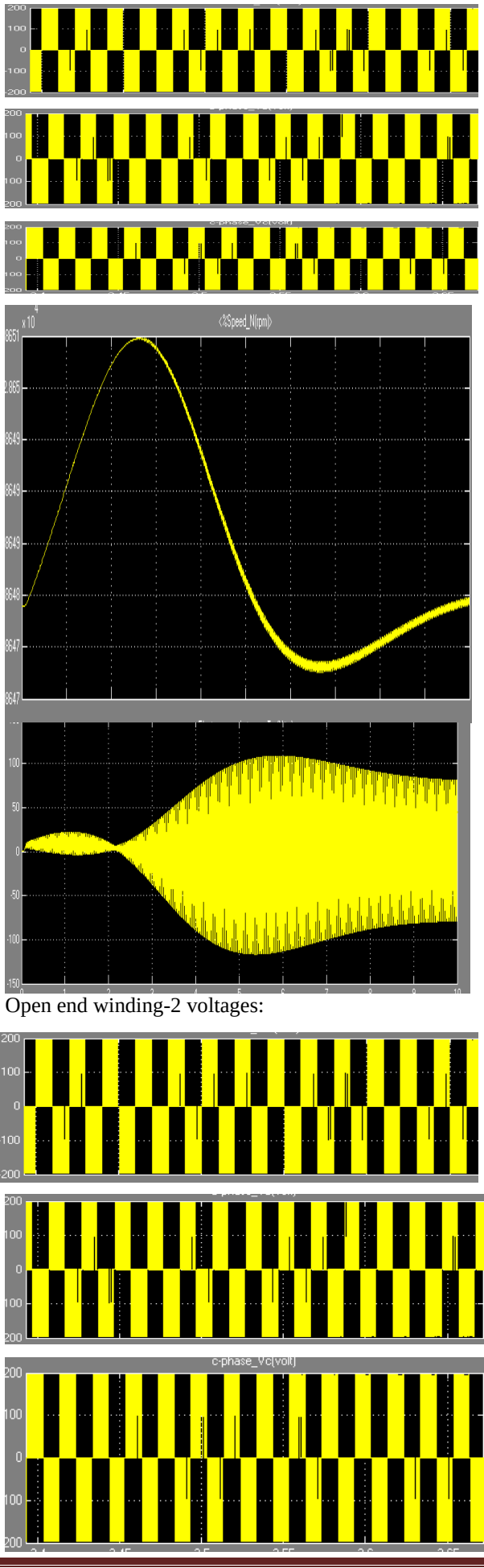

Open end winding-2 voltages:

CONCLUSION

In this paper, an integrated single-stage solution of PV-fed pump drive is presented. The proposed system has the feature of low dc-bus voltage requirement, MPPT integrated with *V/f*, three-level inverter operation and low cost. Analytical proof for low dc-bus voltage requirement in the proposed system is presented.

Implementation of *V/f* with MPPT can be verified with simulation and experimental results. Thus, a high-performance integrated solution is proposed. Low cost of the proposed system can be attributed to the requirement of low voltage dc-link bus capacitor, low voltage rating switches, and less number of sensors for the integrated control operation which is presented in Table II. Thus, in all, this paper presents one of the effective and simple solutions for PV power-fed water-pump application.

REFERENCES

[1] D. Maheswaran, K. K. Jembu Kailas, V. Rangaraj, and W. Adithya Kumar, "Energy efficiency in electrical systems," in *Proc. IEEE Int. Conf. Power Elect. Drives Energy Syst.*, Dec. 2012, pp. 1–6.

[2] Y. Yao, P. Bustamante, and R. S. Ramshaw, "Improvement of induction motor drive systems supplied by photovoltaic arrays with frequency control," *IEEE Trans. Energy Convers.*, vol. 9, no. 2, pp. 256–262, Jun. 1994.

[3] J. V. Mapurunga Caracas, G. de Carvalho Farias, L. F. Moreira Teixeira, and L. A. de Souza Ribeiro, "Implementation of a high-efficiency, high lifetime and low-cost converter for an autonomous photovoltaic water pumping system," *IEEE Trans. Ind. Appl.*, vol. 50, no. 1, pp. 631–641, Jan./Feb. 2014.

[4] J.Appelbaum, "Starting and steady-state characteristics of dc-motors powered by solar cell generators," *IEEE Trans. Energy Convers.*, vol. EC-1, no. 1, pp. 17–25, Mar. 1986.

[5] S. M. Alghuwainem, "Steady-state performance of DC motors supplied from photovoltaic generators with step-up converter," *IEEE Trans. Energy Convers.*, vol. 7, no. 2, pp. 267–272, Jun. 1992.

[6] S. R. Bhat, A. Pittet, and B. S. Sonde, "Performance optimization of induction motor-pump system using photovoltaic energy source," *IEEE Trans. Ind. Appl.*, vol. IA-23, no. 6, pp. 995–1000, Nov./Dec. 1987.

[7] M. A. Vitorino and M. B. de Rossiter Corrˆea, "An effective induction motor control for photovoltaic pumping," *IEEE Trans. Ind. Electron.*, vol. 58, no. 4, pp. 1162–1170, Apr. 2011.

[8] S. Jain and V. Agarwal, "A single-stage grid-connected inverter topology for solar PV systems with maximum power point tracking," *IEEE Trans. Power Electron.*, vol. 22, no. 5, pp. 1928–1940, Sep. 2007.

[9] L.H. S. C. Barreto, P. Peixoto Prac, D. S. Oliveira Jr., and R. N. A. L. Silva, "High-voltage gain boost converter based on three-state commutation cell for battery charging using PV panels in a single conversion stage," *IEEE Trans. Power Electron.*, vol. 29, no. 1, pp. 150–158, Jan. 2014.

[10] M. A. Herr´an, J. R. Fischer, S. A. Gonz´alez, M. G. Judewicz, and D. O. Carrica, "Adaptive dead-time compensation for grid-connected PWM inverters of single-stage PV systems," *IEEE Trans. Power Electron.*, vol. 28, no. 6, pp. 2816–2825, Jun. 2013.

[11] B. N. Alajmi, K. H. Ahmed, G. P. Adam, and B. W. Williams "Singlephase single-stage transformer less grid-connected PV system," *IEEE Trans. Power Electron.*, vol. 28, no. 6, pp. 2664–2676, Jun. 2013.

[12] Y. Zhou and W. Huang, "Single-stage boost inverter with coupled inductor," *IEEE Trans. Power Electron.*, vol. 27, no. 4, pp. 1885–1893, Apr. 2012.

[13] S. Danyali, S. H. Hosseini, and G. B. Gharehpetian "New extendable single-stage multi-input dc-dc/ac boost converter," *IEEE Trans. Power Electron.*, vol. 29, no. 2, pp. 775–788, Feb. 2014.

[14] E. Muljadi, "PV water pumping with a peak-power tracker using a simple six-step square-wave inverter," *IEEE Trans. Ind. Appl.*, vol. 33, no. 3, pp. 714–721, May/Jun. 1997.

[15] M. Makhlouf, F.Messai, andH. Benalla, "Vectorial command of induction motor pumping system supplied by a photovoltaic generator," *J. Elect. Eng.*, vol. 62, no. 1, pp. 3–10, 2011.